Interfacial superconductivity in semiconducting monochalcogenide superlattices

N. Ya. Fogel,[1,2] E. I. Buchstab,[2] Yu. V. Bomze,[3] O. I. Yuzephovich,[3] A. Yu. Sipatov,[4] E. A. Pashitskii,[1,5] A. Danilov,[6]
V. Langer,[7] R. I. Shekhter,[1] and M. Jonson[1]

[1]*Department of Applied Physics, Chalmers University of Technology and Goteborg University, SE-41296, Goteborg, Sweden*
[2]*Solid State Institute, Technion, 32100, Haifa, Israel*
[3]*B. Verkin Institute for Low Temperature Physics and Engineering, 47 Lenin Avenue, 61164 Kharkov, Ukraine*
[4]*Kharkov Polytechnic Institute, 27 Frunze Street, 61002 Kharkov, Ukraine*
[5]*Institute of Physics, 46 Nauki Avenue, 01028 Kiev, Ukraine*
[6]*Department of Microelectronics and Nanoscience, Chalmers University of Technology and Goteborg University,
SE-41296, Goteborg, Sweden*
[7]*Department of Inorganic Environm. Chemistry, Chalmers University of Technology and Goteborg University,
SE-41296, Goteborg, Sweden*

Superconducting and structural properties of superconducting semiconducting multilayers are investigated. These layered systems are obtained by epitaxial growth of the isomorphic monochalcogenides of Pb, Sn, and rare-earth elements on a KCl substrate. Some of these compounds are narrow-gap semiconductors (PbTe, PbS, PbSe, SnTe). Layered structures containing one or two narrow-gap semiconductors have a metallic type of conductivity and a transition to a superconducting state at temperatures in the range of 2.5–6 K. Structures containing only wide-gap semiconductors (YbS, EuS, EuSe) do not demonstrate such properties. All superconducting layered systems are type-II superconductors. The critical magnetic fields and the resistive behavior in the mixed state reveal features characteristic of other layered superconductors. However, data obtained in magnetic fields testify that the period of the superstructure corresponds to half of that obtained from x-ray-diffractometry investigations. This is evidence that the superconducting layers in these samples are confined to the interfaces between two semiconductors. Electron microscopy studies reveal that in the case of epitaxial growth the interfaces contain regular grids of misfit dislocations covering all the interface area. These samples appear to undergo a superconducting transition if they have a metallic type of conductivity in the normal state. Samples with island-type dislocation grids only reveal partial superconducting transitions. The correlations between the appearance of superconductivity and the presence of dislocations, which have been found experimentally, lead to the conclusion that the normal metallic conductivity as well as the superconductivity are induced by the elastic deformation fields created by the misfit dislocation grids. A theoretical model is proposed for the description of the narrow-gap semiconductor metallization, which is due to a band inversion effect and the appearance of electron- or hole-type inversion layers near the interfaces. For different combinations of the semiconductors, such inversion layers in the superlattices can have different shapes and topology. In particular, they can form multiply connected periodic nets having a repetition period coinciding with that of the dislocation grids. Numerical estimates show that such a scenario for the appearance of superconductivity is quite likely. It is shown that the new type of metallic and superconducting nanoscale two-dimensional structures with unusual properties may be obtained from monochalcogenide semiconductors.

I. INTRODUCTION

One of the evident trends in modern nanotechnological efforts is the fabrication of composite materials, intentionally designed on the nanometer length scale. Such combinations of materials with different intrinsic properties (electrical and heat conductivity, magnetic or superconducting ordering, elasticity) appear to have unusual characteristics due to a strong mesoscopic behavior caused by the nanometer-ranged spatial scale of the constituting substances. Self-assembled metal-organic composites,[1] structures based on carbon nanotubes[2] and fullerenes,[3] as well as nanoelectromechanical systems[4] are examples of the success of the above efforts. The very fact that such composites are both mechanically heteroelastic and electrically heteroconducting opens the possibility for interplay between electronic and mechanical degrees of freedom, leading to phenomena caused by nano-electromechanical dynamics in the normal and superconducting structures.[5,6]

It is possible to create composites whose elastic and conducting properties vary periodically on the nanoscale even without nanotechnological means, if one deals with specific kinds of materials. This concerns, in particular, three-dimensional superlattices (SL's), consisting of semiconducting NaCl-type cubic monochalcogenides of different metals, which have been grown epitaxially. The modulation of the SL physical characteristics in the direction orthogonal to the layers arises due to the alternate condensation of two semiconductors. The modulation in the plane of the layers is due to the appearance of regular grids of edge misfit dislocations (EMD's) on the interfaces between two isomorphic compounds.[7] It has been known for a long time that the superlattices PbTe/PbS and PbTe/SnTe reveal superconducting transitions,[8–10] though they contain only semiconducting materials. The appearance of superconductivity in these SL's

seems rather remarkable because it is inherent only to the multilayered compositions, while the individual materials constituting the SL's are not superconductors (with the only exception of SnTe having the very low T_c value of 0.22 K (Ref. 11). Single thin films of Pb and Sn chalcogenides with a thickness $d = 150–300$ nm, prepared under the same conditions as the multilayered samples, do not reveal superconductivity either.[12] This raises a question about the origin of superconductivity in semiconducting SL's. The suggestions answering this question are rather controversial,[8–10,12,13] and none of them can be considered as satisfactory up to date, especially due to the scarcity of existing experimental data. Listing the possible explanations, one should start from a rather trivial assumption that superconductivity in the mentioned SL's originates from Pb precipitates.[8] This explanation cannot be excluded for those particular multilayers investigated in Ref. 8, because of the specific method of sample preparation (extra Pb was condensed simultaneously with semiconductors).

In Ref. 10 the superconductivity of a PbTe/PbS system was explained as a strain-induced effect, which arises due to the pseudomorphic conditions at the interface of two films, which lead to the appearance of interfacial metallic electronic states. However, the authors did not take into account the appearance on the interfaces of crystals with different lattice parameters of misfit dislocation grids eliminating pseudomorphic conditions. The exotic excitonic pairing mechanism[14,15] was exploited as another suggestion for the explanation of superconductivity in semiconducting SL's.[10]

In Refs. 9, 12, 13, and 16 the regular grids of the misfit dislocations appearing on the interfaces of the epitaxial PbTe/PbS SL's were regarded as a phenomenon related to the superconductivity. Attempts to find superconducting semiconducting compositions were made recently which were based on the mentioned assumption that the main role in the appearance of superconductivity in semiconducting layered systems belongs to the interfacial EMD grids.

The idea has turned out to be rather fruitful. The superconductivity has been discovered in four semiconducting layered systems: PbS/PbSe, PbS/YbS, PbTe/YbS, and PbSe/EuS.[16] The values of T_c in these SL's are in the range 2.5–6.4 K. The choice of these semiconductors was associated with the fact that all compounds mentioned are isomorphic, and interfacial misfit dislocations should appear during the epitaxial growth of the alternating layers of these materials. Among them there are even the compositions including wide-gap semiconductors EuS and YbS.

In the present work the superconducting and structural properties of the semiconducting superlattices have been studied. We also report on the discovery of one additional superconducting semiconducting superlattice PbTe/PbSe. We have demonstrated experimentally that superconductivity is unambiguously associated with the formation of periodic two-dimensional walls of EMD's near the interfaces, and the superconductivity appears due to the metallization of the surface layers in narrow-gap semiconductors PbS, PbTe, PbSe, and SnTe in the nonhomogeneous elastic deformation fields. Owing to the strong dependence of the width of the forbidden band E_g on the pressure in such semiconductors, a band

inversion takes place. Electron- or hole-type conducting inversion layers (depending on the Fermi-level position in the SL) emerge under the influence of nonuniform elastic deformations induced by periodic grids of EMD's. These layers form either multiconnected nets or isolated nanoscale regions with metallic conductivity. It is assumed that in such inversion layers superconductivity arises due to electron-phonon interaction involving both bulk and surface (interface) acoustic- and optical-phonon modes. Experimental and theoretical proofs in favor of the above-mentioned mechanism of superconductivity in semiconducting SL's are presented. A short report on part of the experimental data presented here was published in Ref. 16.

II. EXPERIMENTAL DETAILS

All investigated layered semiconducting samples consisted of monochalcogenides of lead, tin, and rare-earth metals, which have a NaCl-type cubic crystal structure. The epitaxial multilayers PbTe/PbS, PbTe/PbSe, and PbS/PbSe have been grown by thermal evaporation of the components from tungsten boats with their sequential condensation on a substrate heated up to a temperature of 520–570 K. The samples have been prepared in an oil-free vacuum of $\sim 10^{-6}$ Torr. In the majority of the experiments the cleaved (001) surface of KCl single crystals was used as a substrate. This choice of substrate, also having a NaCl-type crystal structure, guaranteed the epitaxial growth of all multilayered compositions. Some of the PbTe/PbS samples were also condensed on the (001) face of mica. In the case of compositions containing SnTe or monochalcogenides of the rare-earth metals, an electron-beam evaporation technique was employed for the preparation of the samples. All SL's contained ten bilayers. Two-and three-layered sandwiches were prepared as well. The necessity to study properties of sandwiches was dictated, first of all, by the fact that for the epitaxial chalcogenide heterostructures the problem of structural stability is very serious. Their degradation is mainly caused by elastic stresses arising around the interfaces.[17] It was observed that if the sample contains a small amount of interfaces a quick degradation is less probable. This is the reason why, for some combinations of semiconductors, low-temperature measurements were successfully performed only on three-layered sandwiches. Sandwiches with a total thickness not exceeding 150 nm have been used also for the transmission electron microscopy (TEM) studies.

Single films of the narrow-gap semiconductors PbTe, PbS, and PbSe were also produced for the control experiments. Their thickness was in the range of 100–600 nm. None of them revealed any trace of superconductivity. This observation excludes the possibility that individual semiconducting thin layers in SL's are themselves superconducting.

The layer thickness and the condensation rate have been monitored *in situ* by quartz resonators. In the case of relatively small layer thicknesses (15–40 nm) the superlattice wavelengths and their regularity have been checked by x-ray diffraction. All the rocking curves contain three narrow satellite peaks of first, second, and third orders. A characteristic rocking curve for the PbTe/PbS SL is presented in Ref. 12.

TABLE I. Parameters of the semiconducting SL's with different combinations of components.

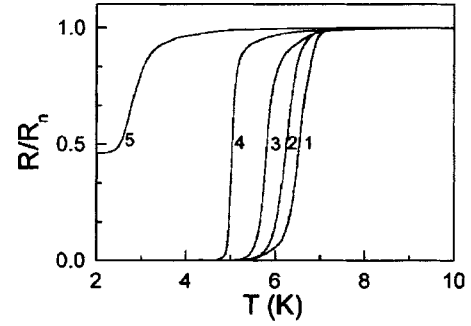| System	Misfit f (%)	D_g, nm (calc)	D_g, nm (exper)	T_c, K
PbTe/PbS	8.3	5.2	5.2	6.03
PbTe/SnTe	2.0	23.0	23–25	2.97
PbTe/PbSe	5.1	8.6	8.6	6.02
PbS/PbSe	3.16	13.5	13.5–14	4.59
PbTe/YbS	13	3.3	3.3	5.93
PbS/YbS	4.8	8.5	8.5–8.8	6.39
PbSe/EuS	2.5	17.0	18.0	2.48
YbS/EuS	5.3	7.7	7.7–7.8	No
YbS/YbSe	3.83	10.6	11–12	supercond.

FIG. 1. The resistive transitions at $H=0$ on the epitaxial PbTe/PbS SL's and sandwiches. (1) three-layer sandwich, $d_{1,2}=250$ nm, (2) asymmetric SL, $d_{\text{PbTe}}=12$ nm, $d_{\text{PbS}}=500$ nm; (3) symmetric SL, $d_{1,2}=50$ nm; (4) symmetric SL, $d_{1,2}=35$ nm; (5) symmetric SL, $d_{1,2}=7.5$ nm.

III. EXPERIMENTAL RESULTS

A. Resistance and transition temperatures

1. Resistive superconducting transition at $H=0$ and resistivity in a normal state

The crystal structure of the multilayers was studied in the θ-2θ geometry using Cu-K radiation on a Siemens D 5000 diffractometer. The TEM and electron-diffraction investigations have been carried out with EVM-100 AK electron microscope with a resolution of 1 nm.

For the most stable PbTe/PbS system the thickness of PbS semiconducting layers has been varied in a range 5–500 nm, the one of PbTe—in a range 5–60 nm. Along with "symmetric" SL's with the equal thicknesses of the both layers $d_1 = d_2$ and the three-layer sandwiches, two series of the samples have been prepared: a series with the constant $d_{\text{PbTe}} = 12$ nm and variable d_{PbS}; a series with the constant $d_{\text{PbS}} = 12$ nm and variable d_{PbTe}.

In the case of other compositions two sets of the samples were prepared: (1) SL's and three-layered sandwiches with equal thicknesses of both the semiconducting layers $d_1 = d_2 = 100 \pm 10$ nm; and (2) two- and three-layer sandwiches with a total sample thickness no more than 150 nm, which were prepared mostly for TEM investigations. The list of the system studied is presented in Table I.

Transport measurements were performed in a standard helium cryostat equipped with a 5-T superconducting coil. The orientation of the sample in a magnetic field was changed with the help of a special rotation mechanism. The accuracy of the determination of the angle between the applied magnetic field **H** and the layer planes was no worse than 0.1°. At the rotation of the sample the transport current was always perpendicular to the applied magnetic field. The parallel orientation was identified by finding the minimum resistance. The stabilization of the temperature at a given point was about 10^{-3} K. The critical magnetic fields were defined from the resistive transitions by the criterion $R = 0.5R_n$. The resistance measurements were carried out using standard four-probe technique with a transport current of 100 μA.

The normal resistance of all samples was in a range 4–200 Ω (the only exceptions were the samples containing two wide-gap semiconductors for which the normal resistance was several kΩ). On the different samples we were able to detect the values of $R/R_n = 2.10^{-4} - 5.10^{-6}$.

Typical resistive transitions into the superconducting state for the epitaxial PbS/PbTe SL's and sandwiches prepared on KCl substrates are shown in Fig. 1. As a rule, these transitions are rather sharp, and the transition width, as defined by the range $(0.1-0.9)R_n$, is about a few tenths of a K. Only for SL's with relatively thin layers ($d_{1,2} < 7-8$ nm) are the transitions of an essentially different kind. They appear to be rather wide and uncompleted (see curve 5 in Fig. 1). For the superlattices with a layer thickness <5 nm even traces of superconductivity do not appear in the temperature range accessible to us. We will further refer to samples that do not reveal superconductivity at $T > 1.5$ K as nonsuperconducting samples.

A very different behavior of the resistive transitions has been observed for SL's condensed on mica. In these samples, independently of the semiconducting layer thicknesses, only partial resistive transitions, if any, have been found. The resistance reduction has been about 15–30 % of the resistivity in the normal state. There is an obvious similarity between the resistive transitions in the latter samples and in SL's with thin semiconducting layers. Further we will mainly consider the data for entirely superconducting SL's. However, as will be shown below, the results for partially superconducting samples are also important for understanding the mechanism of superconductivity in the monochalcogenide layered systems.

The temperature dependence of the resistance for different semiconducting heterostructures for the extended range of T is shown in Fig. 2. It must be emphasized that a metallic-type conductivity was observed for all layered samples revealing a superconducting transition. For the majority of the semiconducting heterostructures the resistance ratio $r = R_{300 \text{ K}}/R_n$ varies in a range 1.5–6. No correlations between T_c and r for these samples was found. The ratio $r < 1$ was obtained for only few PbTe/PbS samples, and these SL's were nonsuperconducting. Thus a metallic-type conductivity
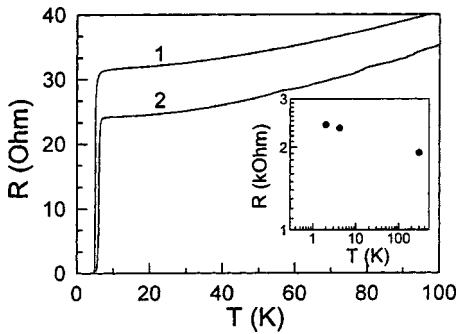
FIG. 2. The resistance as a function of the temperature for SL's with different combinations of semiconductors in the extended range of temperatures. (1) PbTe/PbS. (2) PbS/PbSe. Both SL's are symmetric, with a layer thickness of 100 nm. Inset: the resistance as a function of temperature for a YbS/EuS SL.

is a necessary condition for the appearance of superconductivity.

Figure 2 demonstrates the temperature dependence of the resistance for a SL consisting only of wide-gap semiconductors. Such samples, independently of the type of conductivity, do not reveal superconductivity.

2. Superconducting transition temperatures

The dependence of the superconducting transition temperature T_c on the thickness of the semiconducting layers was investigated on PbTe/PbS system. This study enabled us to make the correct choice of the necessary layer thickness upon further attempts to find superconductivity in other semiconductor multilayered compositions. Figure 3 shows the T_c dependence on the thickness d_{PbS} of the PbS layer for samples PbTe/PbS. In this figure the data for different types of samples (symmetric SL's with $d_{PbS} = d_{PbTe}$, asymmetric ones with $d_{PbS} \neq d_{PbTe}$ and sandwiches) are shown. There is a steep T_c increase in the d_{PbS} range 7.5–20 nm. At $d_{PbS} > 50$ nm the transition temperature shows a tendency toward saturation. Figure 3 shows that the T_c's for different types of samples practically coincide. This is an important observation because, due to the various stabilities of different compound combinations, we will need to further compare the
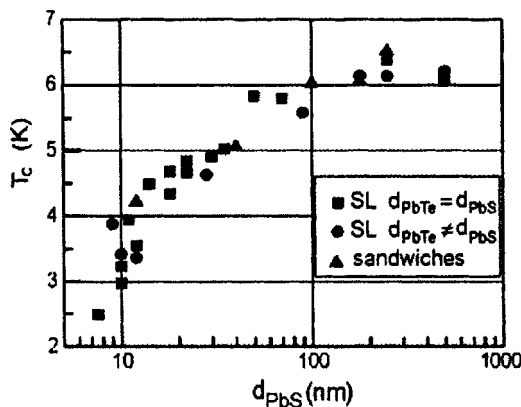

FIG. 3. Transition temperature as a function of d_{PbS} for PbTe/PbS layered samples.
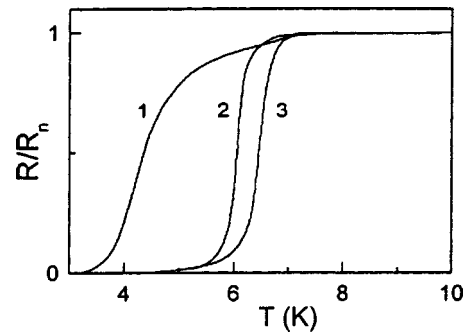

FIG. 4. Resistive transitions at $H=0$ on the epitaxial SL's and sandwiches. (1) PbS/PbSe. (2) PbTe/PbSe. (3) PbS/YbS. The layer thicknesses in all samples are 100 nm.

transition temperatures of the samples with various amount of the layers. The T_c's of the asymmetric SL's and sandwiches with the constant value of $d_{PbS} = 12$ nm and variable d_{PbTe} are practically independent of d_{PbTe} at least in a range 10–60 nm.

Taking into account the results described above for a PbTe/PbS system, we investigated the properties of SL's and sandwiches of different compositions with equal thicknesses of two semiconducting films ($d_1 = d_2 = 100 \pm 10$ nm). How the resistance ratio $R/R_{10 K}$ depends on temperature for some heterostructures prepared on KCl substrates is shown in Fig. 4. A list of the semiconducting heterostructures investigated and the values of T_c obtained are presented in Table I.

B. Critical magnetic fields

Investigations of the critical magnetic fields for different orientations of **H** with respect to the layer planes were mainly performed on symmetric PbTe/PbS SL's with the wavelengths in a range 20–45 nm. The perpendicular critical fields have been measured on some of the asymmetric SL's as well. Results concerning the critical fields were also obtained for PbS/YbS samples.

The resistive transitions in a magnetic field at any field orientation with respect to the layer planes are considerably smeared. Such a smearing is clearly seen in Fig. 5, where data for a PbTe/PbS SL with a wavelength of 23 nm are presented for a perpendicular magnetic field. In the case of
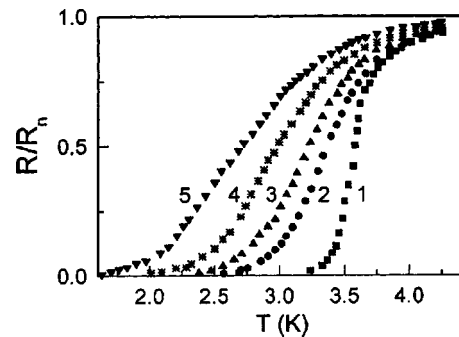

FIG. 5. R/R_n as a function of temperature for a symmetric PbTe/PbS SL with a wavelength $D=23$ nm in different magnetic fields. **H** is perpendicular to the layers. The H values in kOe: (1) 0, (2) 0.14, (3) 0.29, (4) 0.57, and (5) 0.95.
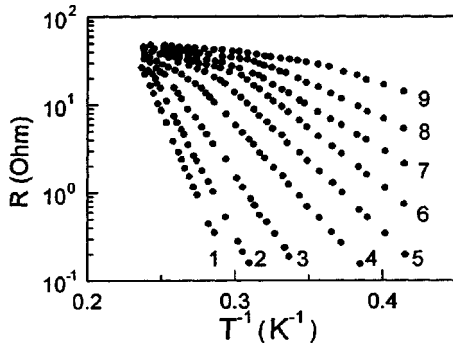
FIG. 6. Resistance as a function of T^{-1} for the symmetric PbTe/PbS SL with a wavelength $D = 37$ nm in different magnetic fields. **H** is perpendicular to the layers. The H values an in kOe: (1) 0.17, (2) 0.25, (3) 0.43, (4) 0.72, (5) 1.02, (6) 1.33, (7) 1.7, (8) 2.2, and (9) 3.0.

FIG. 7. Critical magnetic fields as a function of temperature for a symmetric PbTe/PbS SL. $D = 37$ nm.

the perpendicular field the transition broadening is much stronger than in a parallel field. The features of these transitions are very similar to ones usually observed in high-T_c superconductors and conventional superlattices. For layered superconductors the large broadening of the resistive transitions has been the subject of numerous experiments and theoretical considerations. This behavior was related to the giant magnetic flux creep in the mixed state, which gives rise to a temperature dependence of the resistivity of the thermally-activation type, $R = R_o \exp(-U/kT)$ (see, for example, Ref. 18). Here U is activation energy. Figure 6 shows that Arrhenius plots perfectly describe the dependencies $R(T)$ in the perpendicular magnetic fields. Similar data are obtained for other samples. For PbTe/PbS SL's the activation energy is $U \sim H^{-1/2}$, like for some of HTS compounds and conventional SL's.[19] However, the activation energy is about 10^2 times less than in high-T_c materials.

An analogy with the results obtained for HTS materials is also observed in the experimental data for the resistive transitions in tilted magnetic fields. For a wide range of the angles (30°–90°) there is a scaling of the resistive transitions when the resistance is plotted as a function of $H \sin \varphi$ (the angle φ is equal to 0° if the field is parallel to the layer planes). Such an angular scaling behavior, which was previously seen for YBCO and BSCCO crystals,[20] has been explained by the authors as a consequence of the independent response of the tilted vortex structure on the parallel and perpendicular components of a magnetic field,[21] when these vortices consist of short two-dimensional pancakes joined together by the Josephson strings. The broadening of the transitions is essentially anisotropic, again as in high-T_c materials.

The magnetic critical fields $H_{c\perp}$ and $H_{c\parallel}$ determined by the midpoints of the resistive transitions are presented in Fig. 7 as functions of temperature. Because of the close similarity in the properties of the semiconducting SL's investigated and the HTS behavior, one encounters the same difficulties as in a case of high-T_c superconductors. The critical field values and the derivatives dH_{c2}/dT depend markedly on the R/R_n level which was used for their determination. Nevertheless, results obtained in such a way are sufficiently reliable be-
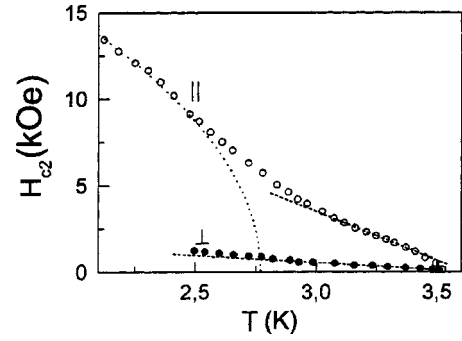
cause the main features of the $H_{c2}(T)$ behavior, and the γ values do not depend on the R/R_n level. Figure 7 demonstrates, first of all, the significant anisotropy of the critical magnetic fields. Anisotropy is present for all samples investigated, and the values of the anisotropy parameter γ for different multilayers are in a range 4–10. The $H_{c\parallel}(T)$ dependence is linear in the vicinity of T_c, i.e., $H_{c\parallel} \sim (T_c - T)$; at lower temperatures this dependence becomes square-root-like: $H_{c\parallel} \sim (T_{cx} - T)^{1/2}$ [T_{cx} is a so-named extrapolation transition temperature, which is usually lower than T_c (Ref. 22)]. Such a dependence means that the crossover from a three-dimensional (3D) to a 2D behavior takes place when the temperature is lowered. Dimensional crossover was observed on many artificial SL's of different type.[23]

The qualitative similarity of the data obtained to those found in conventional SL's and large γ values allow one to state that semiconducting samples investigated consist of the superconducting layers separated by non-superconducting interlayers. From the data obtained in a range of 2D behavior one can estimate the thickness of the superconducting layers in SL's using the expression $d^2 = 6\Phi_0 H_{c\perp}/\pi H_{c\parallel}^2$. For the samples investigated this thickness is in the interval 12–22 nm.

So far the properties of superconducting semiconducting SL's in magnetic fields are very similar to those observed on other layered superconducting systems. However, a more careful inspection of the critical field data indicates that some essential distinctions from the behavior typical for SL's takes place as well. The $H_{c\perp}(T)$ dependencies (Fig. 7) are linear near T_c, but at low temperatures they acquire a considerable positive curvature.

An essentially more dramatic difference from conventional SL behavior reveals itself in a case of the parallel critical fields.[12] These results are obtained on symmetric PbTe/PbS SL's with $d_1 = d_2 \leq 40$ nm. Having the critical field dependencies on the temperature for two main field orientations, one may easily determine the anisotropy parameter $\gamma = (M/m)^{1/2}$ in three independent ways with the aid of the formulas[22]

$$\gamma = (dH_{c\parallel}/dT)/(dH_{c\perp}/dT), \quad (1)$$

$$\gamma = [\xi(0)/D]\sqrt{T_c/(T_c - \tilde{T}_c)}, \quad (2)$$

$$\gamma = \Phi_0/\pi H_{cr}D^2. \quad (3)$$

Here Φ_0 is the magnetic flux quantum, $D = d_1 + d_2$ is the superstructure period, and H_{cr} is the crossover field. The first of these formulas determines the anisotropy parameter exclusively through the critical field values and does not contain the SL wavelength D. Formulas (2) and (3) include D alongside the parameters which one obtains from the critical fields. It appears that γ values for all samples investigated, which are determined by the above three formulas, coincide only in a case when one uses the value $D/2 = d_1 = d_2$ as the SL wavelength. This means that the repeating distance between the centers of the superconducting layers is equal to the individual semiconductor film thickness, but not to the bilayer thickness $d_1 + d_2$, as it is for all conventional SL's.[23] In the meantime, the x-ray diffractometry gives the value $D = 2d_{1,2}$, in accordance with the magnitude following from the fabrication process. Thus this observation allows one to make very important conclusions concerning the nature of the superconductivity in semiconducting SL's. Since the superconducting SL wavelength is equal to the individual semiconducting film thickness, it is clear that the superconducting layers are located on the interfaces between two semiconductors.

Also of special interest are the data obtained on the multilayer with the large layer thicknesses of 100 nm in parallel magnetic fields. This sample also displays 2D behavior at low temperatures, i.e., a square-root-like dependence on T. For this sample the superconducting layer thickness is equal to 22 nm, i.e., essentially smaller than that of the constituting semiconducting layers. This confirms the suggestion that the bulk of semiconductors is not in the superconducting state.

The values of the $dH_{c\perp}/dT$ for PbTe/PbS SL's are not very high. Its maximum value obtained until now is about 2 kOe/K, but for many samples it does not exceed 1 kOe/K. Correspondingly, the values of the coherence length $\xi_{\parallel}(T=0)$ obtained from the perpendicular critical fields are in a range 17–40 nm.

C. Crystalline structure

First of all, let us consider the structural features that may be of importance for the explanation of the origin of superconductivity in the semiconducting heterostructures investigated. At the initial stage of the epitaxial growth of a monochalcogenide on the "substrate" from another monochalcogenide according to the Franck–van der Merwe mechanism, the growing film acquires the same structure as the "substrate," with the interatomic distance coinciding with that of substrate. It is so-called pseudomorphic stage of growth. On this stage a large strain in the growing layer as well as in the substrate is accumulated. One of the materials, having a larger lattice parameter a, appears to be compressed; another one with a smaller a is expanded.

The value of the stresses depends on the misfit parameter $f = 2(a_1 - a_2)/(a_1 + a_2)$ between the crystal lattice parameters a_1 and a_2 in the two compounds. However, when the thickness of the growing layer exceeds some critical magnitude d_c depending on the compound combination, the partial stress relaxation takes place due to the formation of misfit dislocations or, in a less favorable case, due to the mechani-
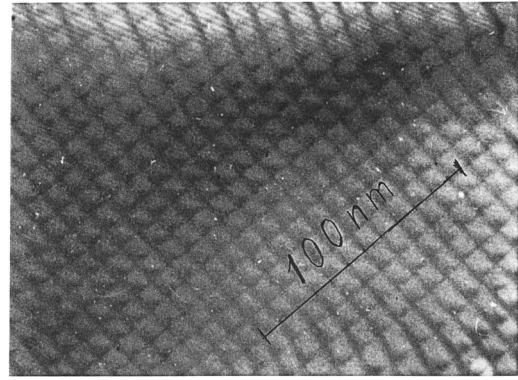

FIG. 8. The dislocation grid in the PbTe/PbSe two-layer sandwich.

cal destruction of the sample.[17] The stresses essentially decrease with the appearance of the misfit dislocations, but the complete relaxation of the stress as a rule cannot be attained.[24] The less the misfit f, the higher the level of the stress until rather large d.[24] For heterostructures with a small amount of layers the risk of the destructive scenario of the structure transformation becomes less likely. This is the reason why, for some compositions, only three-layer sandwiches were successfully tested for superconductivity.

Misfit dislocation system forms a regular square grid. The period of this grid D_g is determined by the formula[7]

$$D_g = b/f. \qquad (4)$$

Here b is a projection of the edge component of misfit dislocation Burgers vector on the interface. The experimental picture demonstrating the typical view of the dislocation grid is shown in Fig. 8.

The values of the misfit parameter f calculated for the different combinations of the compounds are presented in Table I. This table also contains the experimental values of the dislocation grid periods D_g obtained from TEM investigations for different combinations of semiconductors. In another column of Table I the values of D_g calculated from expression (4) are listed. It appears that experimental and calculated values of D_g are in a fairly good accordance.

The critical thickness for the appearance of the misfit dislocations, as mentioned, depends on the misfit between lattice parameters in two contacting compounds. For the combination PbTe/PbS with the misfit parameter $f = 8.3\%$ it is about 2 nm, while in the heterostructure PbS/EuS with $f = 0.5\%$ pseudomorphic growth occurs up to a thickness essentially exceeding 100 nm.[25]

All diffraction data in θ-2θ geometry show that only reflections of ($h00$) type are present for all compounds in the SL's as well as for the KCl substrate. The data of other scan modes, with a fixed incidence beam angle and just detector scanning, allowed us to detect other reflections with indices (hkl), originating from planes not parallel to the layer surface. These data testify that all crystallographic directions in the substrate and in SL components coincide.[26] All the data obtained may be regarded as evidence that SL's condensed on the KCl substrate are perfect single-crystal multilayered

structures. In the case of the samples prepared on mica substrate the SL's consist of blocks with two different orientations (with the directions [100] and [111] perpendicular to the layer planes).

The stability of the semiconducting SL's studied is rather low, and their lifetime during which the samples remain continuous and conducting is very limited. There is a number of reasons leading to the destruction of multilayers. The SL's appear to be destroyed due to the thermocycling connected with low-temperature measurements. The most stable composition is PbTe/PbS. These SL's may hold 10–20 thermocycles without degradation of the structure and superconducting properties. Another reason for the degradation is a mechanical destruction (appearance of cracks penetrating through the depth of the sample), which is due to the elastic stresses. In some cases a partial decomposition of the Pb-containing compounds occurs, and the weak diffraction lines characteristic for polycrystalline Pb appear. In fresh PbTe/PbS SL's the Pb lines are absent, but they appear as a result of the aging during a few months. This corresponds approximately to the superconductivity lifetime in these samples, but a rather large statistics is needed for the statement whether such type decomposition may be directly associated with the destruction of superconductivity. The lines corresponding to the free Pb have never been seen on PbTe/PbSe, PbTe/YbS and PbTe/EuS samples (even after yearlong aging). And at last, the solid state chemical reactions between different elements take place after the long aging. As a result of the aging effect the additional lines appear on the x-ray diffractograms. The majority of these lines may be identified as belonging to compounds of K and S with different valences. The location of these compounds should be close to the interface between the substrate and the first semiconducting layer because, according to Auger electron spectroscopy analysis, no traces of K were observed in several upper layers of the EuS/PbS superlattice.[26]

IV. DISCUSSION AND THE THEORETICAL MODEL

Before discussing the theoretical model proposed here for the explanation of the origin of superconductivity in the purely semiconducting heterostructures let us sum up the main experimental results presented above. We will also discuss all correlations (and anticorrelations) between physical properties and the structure of these SL's.

The PbTe/PbS system was studied most extensively because of its relative stability, and some conclusions made on the basis of these results may be applied to virtually all the semiconducting SL's of the monochalcogenide type. In brief, the results obtained are as follows.

(1) Seven of nine semiconducting SL's investigated are superconductors with T_c in the range 2.5–6.4 K. Superconductivity is not discovered (down to 1.5 K) in two combinations containing only wide-gap semiconductors (YbS/EuS, YbS/YbSe). All SL's containing one or two narrow-gap semiconductors (PbS, PbSe, PbTe, SnTe) reveal superconducting transitions.

(2) All superconducting SL's have a metallic-type conductivity. When a negative temperature coefficient of resistivity
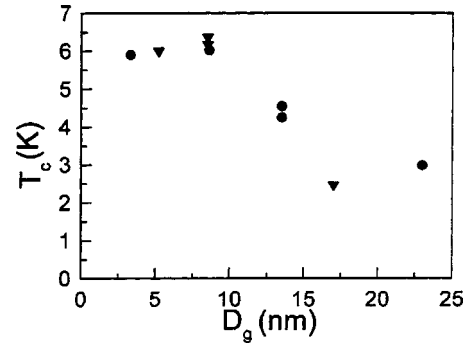

FIG. 9. T_c as a function of the dislocation grid period.

is observed (as in the inset of Fig. 2 for SL's consisting of two wide-gap semiconductors, or for imperfect samples containing narrow-gap semiconductors), there is no superconducting transition.

(3) All layered superconducting samples studied are perfect single crystals, which contain EMD grids on the interfaces between two semiconductor crystals. The single crystallinity is observed in the whole volume of the multilayered samples. In a case when the dislocation grids do not cover the entire area of the interfaces the superconducting transition appears uncomplete, i.e., after a partial phase transition a constant resistance, lower than the residual one, is conserved. These facts most probably imply that superconducting phase may form a disconnected island system. Thus the obvious correlation between superconductivity appearance and its features, on the one hand, and the EMD grid existence, on the other hand, is discovered. The island-type dislocation grids are observed in two cases: (i) at small thickness of the semiconducting layers; and (ii) for the samples condensed on the mica substrate, which does not ensure good epitaxy.

(4) For the superconducting compositions there is a correlation between the values of the transition temperature T_c and the period of the misfit dislocation grid (Fig. 9). When the dislocation density is large (in the D_g range 3.3–8.6 nm) there is practically no dependence of T_c on the interdislocation distance. At $D_g > 10$ nm the reduction of T_c is observed with increasing D_g. These data may be considered as evidence that T_c depends on the density of the dislocations at the interfaces.

(5) It follows from the magnetic critical-field measurements that the systems studied consist of superconducting layers located on the interfaces between two semiconductors separated by the non-superconducting material interlayers. Evidence for this statement follows from the observation of the 3D-2D crossover and the value of the superstructure period $D = d_1 = d_2$ determined above and from large anisotropy parameter γ, which is equal to 4–10 for different samples.

The analysis of the experimental data presented above points out to the important role of the edge misfit dislocations appearing on the interfaces between semiconducting crystals with different lattice parameters. It is found that for combinations of monochalcogenides with a large misfit parameter f and, correspondingly, small periods of the 2D dislocation grid $D_g = b/f$, the values of the superconducting transition temperature T_c are higher. However, there are ex-

ceptions from this rule: the heterostructures YbS/EuS and YbS/YbSe with relatively small D_g (7.7 and 10.6 nm) do not reveal superconductivity. This fact indicates that some additional mechanism along with the presence of the EMD's exists, favoring the appearance of the superconductivity.

It should be emphasized that the metallization and the superconducting phase transition are observed only in such semiconducting heterostructures where one or two of the components are narrow-gap semiconductors (PbTe, PbS, PbSe, SnTe) with a small value of the energy gap [E_g <0.3 eV (Ref. 27)]. These semiconductors also have an anomalously strong dependence of E_g on the pressure. Meanwhile the compounds YbS, YbSe, and EuS are semiconductors with a wide gap ($E_g>1.5$ eV), and they reveal neither metallic, nor superconducting properties.

We are going to show that the appearance of metallic conductivity in semiconducting layered systems may be due to a decrease of the energy gap E_g in narrow-gap semiconductors under influence of the elastic deformations created by the EMD grids near the interphase boundaries. The band bending effect near the interfaces caused by the contact potential difference also makes a contribution to this effect, but it is not so essential as the E_g reduction. The superconductivity in the interfacial metal layers can be explained by the usual BCS pairing which is due to the interaction of the degenerated current carriers (electrons or holes) with the bulk and surface phonons.

According to Ref. 27, at low temperatures ($T=4$ K) the values of the energy gap E_g for the semiconductors PbSe, PbTe, and PbS are small ($E_g=0.165$, 0.190, and 0.286 eV). These compounds are characterized by negative and anomalously large absolute values of the derivatives dE_g/dP (-9.1×10^{-3}, -7.4×10^{-3} and -9.15×10^{-3} eV/kbar, correspondingly). This means that at the pressures $P>10$ kbar the considerable reduction of the energy gap width should be observed. As we will show below, such pressures may arise in the films due to the existence of EMD grids on the interface between the cubic crystals. The Burgers vectors **B** of all the EMD's lie in the boundary plane (x,y), i.e., in a sliding plane. In such a case the elastic stress fields of the individual dislocations in each crystal have the same sign on one side of the boundary (but an opposite sign on the other side of the interface), and they are summed up.

In the framework of the linear elastic theory, one can imagine that the square EMD grid is formed as the superposition of two dislocation walls with the orthogonal to each other directions of the dislocation lines (along axes x and y) having the same periods D_g in both directions. The elastic dilatation of such dislocation grid is a sum of the dilatations of each wall:

$$\varepsilon_i(x,y,z)=\varepsilon_i^\parallel(x,z)+\varepsilon_i^\parallel(y,z), \quad (i=1,2) \qquad (5)$$

Here $\varepsilon_i^\parallel$ (l,z) is a dilatation appearing as a result of the superposition of the elastic deformations of the periodic (along axis $l=y$, x) chains of the EMD's with the Burgers vectors **B** parallel to the sliding plane:[28]

$$\varepsilon_i^\parallel(l,z)=-\frac{|\vec{B}|(1-2\sigma_i)\sinh(2\pi z/D_g)}{2D_g(1-\sigma_i)\coth(2\pi z/D_g)-\cos(2\pi l/D_g)},$$
$$(6)$$

Here σ_i is the Poisson coefficient of the ith crystal. One may easily see from formula (6) that $\varepsilon_i(x,y,z)\to0$ at $z\to0$ in all the points of plane (x,y) except the points along the dislocation lines, on which conditions $\cos(2\pi x/D_g)$ $=\cos(2\pi y/D_g)=1$ is valid. On the other hand, at large distances $|z|\gg D_g/2\pi$ the dilatation $\varepsilon_i(x,y,z)$ approaches a constant limit

$$\varepsilon_i(x,y,|z\to\infty)\equiv\varepsilon_i^\infty=-\frac{|\vec{B}|(1-2\sigma_i)}{D_g(1-\sigma_i)}\,\mathrm{sgn}\,z \qquad (7)$$

which corresponds to the compression of the crystal in the region $z>0$ and to the extension in the region $z<0$. It is worth mentioning that the sign of the periodic elastic dilatation [Eq. (5)] created by the EMD grid in each crystal is opposite to the sign of the initial homogeneous elastic deformation (compression or expansion), which is due to the pseudomorphic growth of the semiconducting films. In Fig. 10 the space distribution of the periodic (along x and y axes) elastic dilatation [Eq. (5)] created by the EMD grid at the definite distance z from the interface plane $z=0$ is shown.

The values of the pressures in ith crystal created by dilatation are equal to

$$P_i=-K_i\varepsilon_i, \quad K_i=E_i/3(1-2\sigma_i), \qquad (8)$$

Here K_i is the compression modulus, and E_i is the Young modulus.

For example, in the cubic crystal PbS with the lattice elastic modulus components $C_{11}=1270$ kbar, C_{12} $=300$ kbar and $C_{44}=250$ kbar,[27] the Poisson coefficient and the compression modulus are equal to 0.32 and 630 kbar, correspondingly. Assuming for PbS the value of $B=a$ $=6$ Å and taking $D_g=5.2$ nm for a contact with PbTe, we obtain, from Eqs. (7) and (8), such estimates: $|\varepsilon_i^\infty|\sim6\ 10^{-2}$ and $|P_i^\infty|\sim38$ kbar (P_i^∞ is the pressure arising in an ith crystal on the distance $z>D_g/2\pi$ from interface). Since the derivative $dE_g/dP=-9.15\times10^{-3}$ eV/kbar in PbS, the decreasing of the energy gap width under this pressure is $\Delta E_g=0.35$ eV and it is larger than the initial ambient gap value $E_g=0.29$ eV. This means that, in such a situation, the band inversion occurs in the crystal PbS.

However, it is necessary to take into account the initial pseudomorphic deformation of a PbS film grown in contact with a PbTe crystal, which has a greater lattice constant (a $=6.13$ Å) than the PbS crystal ($a=5.94$ Å). In the pseudomorphic state, an expansion of the PbS crystal takes place, and a gap widening occurs. The elastic dilatation created by the EMD grid on interface has the opposite sign, and it leads to a compression of the PbS crystal and to a gap narrowing.
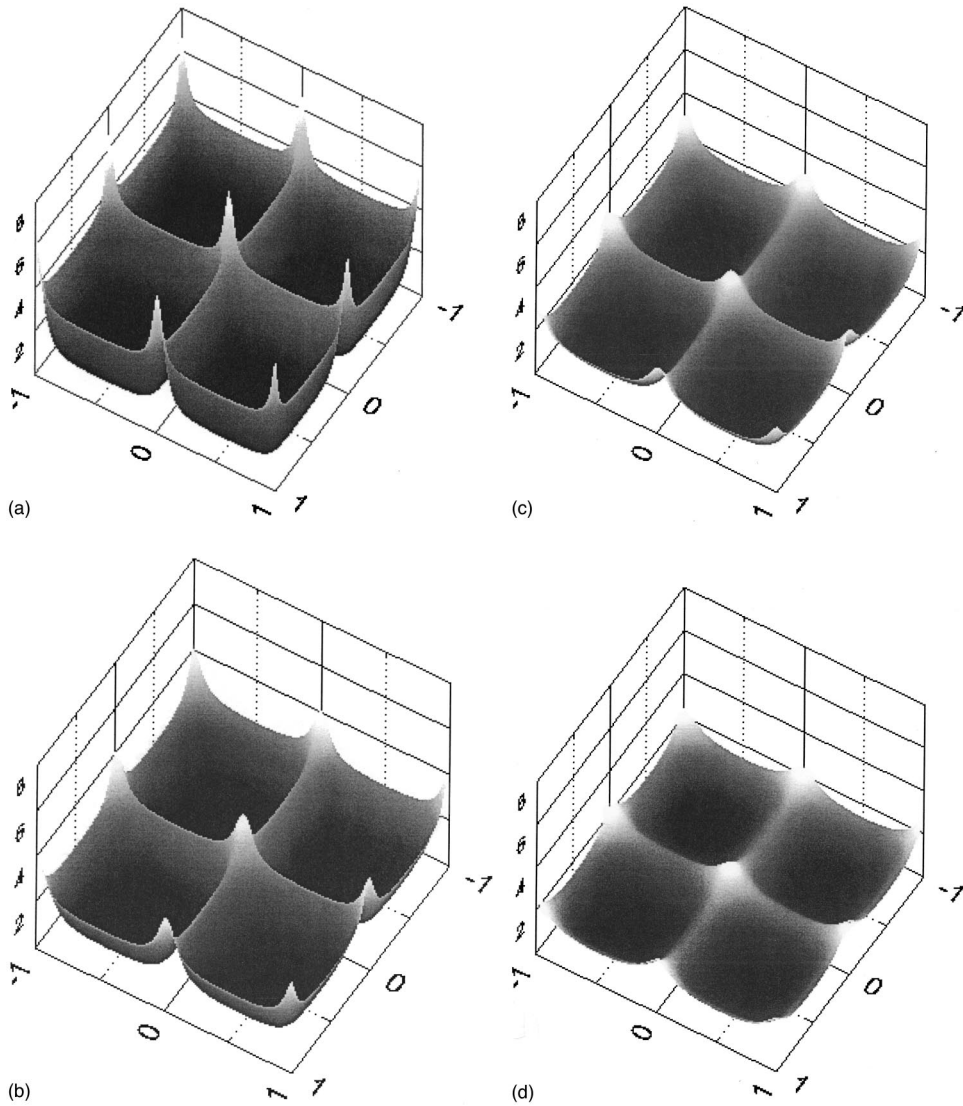
(a)

(b)

(c)

(d)

FIG. 10. The spatial distribution of the elastic deformation of the crystal lattice, which is due to the square EMD grid on an interface between PbS and PbTe, for different distances z from the interface: (a) $z=0.3$ D_g, (b) $z=0.5$ D_g, (c) $z=0.7$ D_g, (d) $z=0.9$ D_g. Deformations are in the arbitrary units, and x and y values are in the units of D_g. The shape of the "landscape" does not change with the increase of z, but the peak height diminishes with $z \rightarrow D_g$.

This dilatation is very strong near the interface, along the EMD lines, where the real effects of the band inversion in semiconductor PbS and the creation of electron-or hole-type inversion layers with metallic conductivity can take place.

As a result, the surface of the band inversion points in the PbS film near interface has a multy-connected periodic shape (see Fig. 11). The metallic inversion layers near this surface form square nanoscale nets with the sizes of the cells equal to D_g. Such a multiply connected structure of conducting and, at $T<T_c$, superconducting nets can lead to unusual properties of the semiconducting SL's, in particular to a quantization of the magnetic field flux both in the normal and superconducting states. The quantum period in magnetic field is $H=ch/eD_g^2$ for the normal metallic net and equal to 6.4 T for $D_g=25$ nm.

At the same time, the pseudomorphic deformation of the PbTe crystal is compression, and this leads to an energy gap reduction. Since the gap in the PbTe semiconductor is very small ($E_g=0.19$ eV), it leads right up to the band inversion, when the gap is negative. In this case, the EMD grid dilatation promotes the reinversion of bands in the bulk, and the
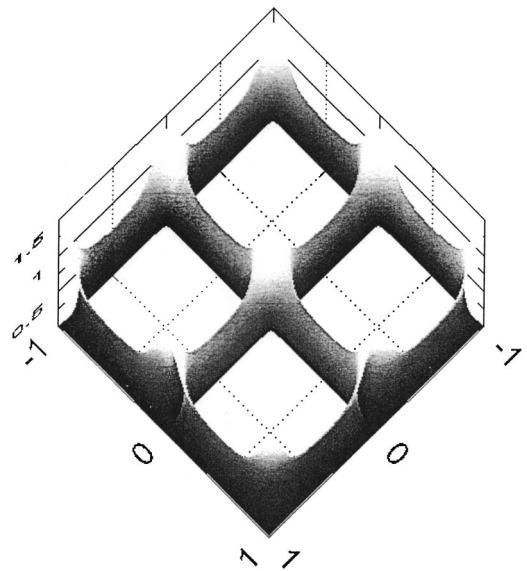

FIG. 11. The multiconnected topology of the surface of the band inversion points in the crystal PbS.

surface of the points, where the gap is equal to zero, touches the interface. Thus an intersection of the metallic inversion layer by the insulating dislocation cores in the interface plane takes place. As a result, this metallic and superconducting layer decomposes into individual separate parts inside the EMD grid cells. This can lead to unusual superconducting properties at $T < T_c$ due to the existence of the 2D square net of Josephson-type weak links along EMD lines. Such nets of weak links can be sensitive to the Josephson vortex dynamics. Since the effective masses of electrons (holes) are sufficiently small, the space quantization of the electron (hole) spectrum in the narrow potential well of the bent bands should take place, i.e., a transition to the case of 2D metal occurs.

In the meantime, the bending of the bands, which is due to the contact electrostatic potential for compounds PbS, PbTe, PbSe, and SnTe, similar in their chemical properties, is not sufficient for the formation of heterostructure with metallized inversion layers on interfaces, in distinction to the systems of $GaAs/Al_xGa_{1-x}As$ type. Beside that, the electrostatic fields are screened strongly due to the very large values of the static dielectric constant in these ionic type crystals [$\varepsilon_0 \approx 2000$ (Ref. 27)].

Superconductivity arising in the metallized inversion layers at the low temperatures most probably is stipulated by the usual mechanism of the Cooper pairing of the degenerated current carriers through the interaction with the acoustic and optical phonons (the BCS model). If the spectrum of electrons (holes) near the interface is weakly quantized and, consequently, is actually three dimensional, the electron-phonon interaction is mainly determined by the bulk phonons in crystals, and the superconducting order parameter is in fact quasi-isotropic.

When the spatial quantization is sufficiently strong (i.e., the distance between neighboring 2D levels $\Delta E > T_c$), the most effective electron-phonon interaction may be connected with the interfacial surface 2D phonon modes[29,30] localized on the interphase boundaries of different crystals. The possibility of superconductivity of 2D electrons, which is due to their interaction with the surface (Rayleigh) phonons, was considered in Ref. 14. In this case the maximal T_c is accessed at the sufficiently low thickness d of the metallic film, that is, when the condition $d < \lambda_s$ is met. Here λ_s is the effective penetration depth of the surface phonon, equal by an order of magnitude to the inverse Fermi wave vector $k_F^{-1} = (2\pi N_s)^{-1/2}$, and N_s is a surface density of the 2D electron gas.

However, in semiconducting SL's one observes another tendency: the transition temperature decreases with decreasing thickness d of the semiconducting films, and "aspires" to the maximal value with increasing d (see Fig. 3). This experimental result testifies again that the volume of the semiconducting films is not involved in the superconducting transition.

According to Eq. (6), the full dilatation [Eq. (5)], as was mentioned above, is equal to zero on the interface at $z = 0$ in all points of the plane (x,y), excluding the dislocation line areas (near the elastically deformed cores of EMD's). The maximal values of the elastic deformation and local pressure are reached at the distances $z > D_g$ from the interface, in average.

Just for these distances, both band inversion and metallic layer creation occur. So, if the thickness of semiconducting film is less than the characteristic length D_g for the certain system, the inversion layers with metallic conductivity and superconductivity are absent or suppressed, while for the thick films with $d > D_g$ such metallic and superconducting layers are fully formed. However, the absence of the complete dislocation nets on the interfaces is even more serious reason for absence of superconductivity at small thickness of the semiconducting layers.

V. SUMMARY

In this paper, the new types of space-periodic nanoscale artificial structures are created and investigated—monochalcogenide semiconducting superlattices with the edge misfit dislocation grids on interfaces, which have metallic and superconducting properties. The temperature dependencies of the resistance and superconducting resistive transitions (if they are present) are studied. For some of the SL's the critical magnetic-field behavior is investigated as well. For the majority of layered systems extensive structural investigations are accomplished. It is shown that the appearance of superconductivity and its features always correlate with properties of the interfaces between two different semiconductors where misfit dislocations are located.

A theoretical model is proposed for a description of narrow-gap semiconductor metallization, which may serve as a basis for explaining the unusual SL properties observed. The metallization of narrow-gap semiconducting films in SL's is a result of the anomalously strong dependence of the energy gap on pressure. This leads to the band inversion effect in narrow-gap semiconductors and to the appearance of electron- or hole-type inversion layers near interfaces with metallic conductivity and superconductivity below the critical temperature $T_c = 2.5 - 6.4$ K. Such inversion layers in semiconducting films can form multiconnected periodic metallic and superconducting nets along EMD lines or the separate local regions inside cells of the EMD grids.

As a result, the unusual properties of semiconducting SL's can be observed, in particular, quantization of the magnetic field flux in normal as well as in superconducting states, and the collective Josephson effect on the square 2D nets of the extended weak links along the insulating EMD cores. One additional superconducting combination (PbTe/PbSe) in a class of monochalcogenide semiconducting superlattices is discovered.

[1] A. Ulman, Chem. Rev. **96**, 1533 (1996).

[2] P. G. Collins, H. Bando, and A. Zetti, Nanotechnology **9**, 153 (1998); S. J. Tans, M. H. Devoret, H. Dai, A. Thess, R. E. Smalley, L. J. Georliga, and C. Dekker, Nature (London) **386**, 474 (1997).

[3] H. Park, J. Park, A. K. L. Lim, E. H. Anderson, A. P. Alivisatos, and P. L. McEuen, Nature (London) **407**, 57 (2000).

[4] A. Erbe, C. Weiss, W. Zwerger, and R. H. Blick, Phys. Rev. Lett. **87**, 096106 (2001).

[5] L. Y. Gorelik, A. Isacsson, M. V. Voinova, B. Kasemo, R. I. Shekhter, and M. Jonson, Phys. Rev. Lett. **80**, 4526 (1998); A. Isacsson, L. Y. Gorelik, M. V. Voinova, B. Kazemo, R. I. Shekhter, and M. Jonson, Physica B **255**, 150 (1998).

[6] L. Y. Gorelik, A. Isacsson, Y. M. Galperin, R. I. Shekhter, and M. Jonson, Nature (London) **411**, 454 (2001).

[7] V. M. Kosevitch and L. S. Palatnik *Electron Microscopic Images of Dislocations and Stacking Faults*, (Nauka, Moscow, 1976).

[8] K. Murase, S. Ishida, S. Takaoka, and T. Okumura, Surf. Sci. **170**, 486 (1986).

[9] O. A. Mironov, A. B. Savitskii, A. Yu. Sipatov, A. I. Fedorenko, A. N. Chirkin, S. V. Chistyakov, and L. P. Shpakovskaya, Pis'ma Zh. Eksp. Tear. Fiz. **48**, 100 (1988) [JETP Lett. **48**, 106 (1988)].

[10] D. Agassi and T. K. Chu, Phys. Status Solidi B **160**, 601 (1990).

[11] R. A. Hein, J. W. Gibson, R. S. Allgaier, B. B. Houston, R. L. Mazelsky, and R. C. Miller, in *International Conference on Low Temperature Physics (LT9)*, edited by J. G. Daunt *et al.* (North-Holland, New York, 1965), p. 604.

[12] I. M. Dmitrenko, N. Ya. Fogel, V. G. Cherkasova, A. I. Fedorenko, and A. Yu. Sipatov, Fiz. Nizk. Temp. **19**, 747 (1993) [Low Temp. Phys. **19**, 533 (1993)].

[13] N. Ya. Fogel, A. I. Erenburg, A. Pokhila, Yu. Bomze, A. Yu. Sipatov, and V. Langer, Physica B **284−288**, 1123 (2000).

[14] V. L. Ginsburg and D. A. Kirzhnits, Usp. Fiz, Nauk. **101**, 185 (1970) [Sov. Phys. Usp. **13**, 335 (1970)].

[15] D. Allender, J. Bray, and J. Bardeen, Phys. Rev. B **7**, 1020 (1973).

[16] N. Ya. Fogel, A. S. Pokhila, Yu. V. Bomze, A. Yu. Sipatov, A. I. Fedorenko, and R. I. Shekhter, Phys. Rev. Lett. **86**, 512 (2001).

[17] L. S. Palatnik and A. I. Fedorenko, J. Cryst. Growth **52**, 917 (1981).

[18] A. P. Malozemoff, Y. Yeshurun, L. Krusin-Elbaum, T. K. Worthington, D. C. Cronemeyer, T. Dinger, T. R. Foltzberg, T. R. McGuire, and P. H. Kes, in *High Temperature Superconductivity*, edited by R. Nikolsky (World Scientific, Singapore, 1988), Vol. 9, p. 112

[19] N. Ya. Fogel, A. Yu. Sipatov, A. I. Fedorenko, V. N. Rybal'chenko, and V. G. Cherkasova, Fiz. Nizk. Temp. **20**, 1142 (1994) [Low Temp. Phys. **20**, 897 (1994)].

[20] H. Raffi, S. Labdi, O. Laborde, and P. Monceau, Phys. Rev. Lett. **66**, 2515 (1991).

[21] P. H. Kes, J. Aarts, V. M. Vinokur, and C. J. van der Beek, Phys. Rev. Lett. **64**, 1063 (1990).

[22] L. I. Glazman, I. M. Dmitrenko, V. L. Tavozhnyanskii, N. Ya. Fogel, and V. G. Cherkasova, Zh. Eksp. Teor. Fiz. **92**, 1461 (1987) [Sov. Phys. JETP **65**, 821 (1987)].

[23] B. Y. Jin and J. B. Ketterson, Adv. Phys. **38**, 189 (1989).

[24] I. F. Mikhailov, B. A. Savitskii, A. Yu. Sipatov, A. I. Fedorenko, and L. P. Shpakovskaya, Kristallography **26**, 792 (1981) [Sov. Phys. Crystallogr. **26**, 449 (1981)].

[25] A. Stachov-Wojcik, T. Story, W. Dobrowolski, M. Arciszewska, R. R. Galazka, M. W. Krejveld, C. H. W. Swuste, H. J. M. Swagten, W. J. M. de Jonge, A. Twardowski, and A. Yu. Sipatov, Phys. Rev. B **60**, 15 220 (1999).

[26] A. I. Erenburg, Yu. V. Bomze, N. Ya. Fogel, A. Yu. Sipatov, A. I. Fedorenko, V. Langer, and M. Norell, Fiz. Nizk. Temp. **27**, 127 (2001) [Low Temp. Phys. **27**, 93 (2001)].

[27] G. Nimitz and B. Schlicht, *Narrow-Gap Semiconductors* (Springer-Verlag, Berlin 1983).

[28] A. Gurevich and E. A. Pashitskii, Phys. Rev. B **56**, 6213 (1997).

[29] Z. V. Popovich, M. Cordona, E. Richter, D. Strauch, L. Tapfer, and K. Ploog, Phys. Rev. B **41**, 5904 (1990).

[30] C. Trallero-Ginev, F. Garcia-Moliner, V. R. Velasco, and M. Cardona, Phys. Rev. B **45**, 11 944 (1992).